As expected, when one of the channels is switched off, Eq. (24) reduces to Eq. (8).

By integrating out ϵ and one of the total widths in Eq. (24) we find that the distribution of the single total width $\Gamma=\Gamma_\lambda/\langle\Gamma_\lambda\rangle$ is given by

$$P(\Gamma)=(\mu_3\pi^{-1})[\exp(\mu_1)][\Gamma(2-\Gamma)-\mu_2]^{-1/2}\times\{\mu_1\mu_3^{-1}[K_1(\mu_1)+K_0(\mu_1)]-2[\Gamma(2-\Gamma)-\mu_2]K_0(\mu_1)\}\times\exp\{-2\mu_3[\Gamma(2-\Gamma)-\mu_2]\},\quad(25)$$

where

$$\mu_1=(\pi/8\langle S\rangle^2)(D_{C1}-D_{C2})^2,\quad \mu_2=4D_{C1}D_{C2}/(D_{C1}+D_{C2})^2,$$
$$\mu_3=(\pi/8\langle S\rangle^2)(D_{C1}+D_{C2})^2.$$

This should be compared with the total dimensionless width y of the R matrix which is given by

$$P(y)=(\pi^{-1})[y(2-y)-\mu_2]^{-1/2}.\quad(26)$$

To compare the distribution of the width Γ given by Eq. (25) with the one given by Eq. (26), we again calculate the mean-square deviations of the quantities Γ and y. As in Sec. II B, we find that the distribution of the width Γ is always broader than the one given by Eq. (26), except when the quantities $D_{C1}/\langle S\rangle$ and $D_{C2}/\langle S\rangle$ are very small.

IV. CONCLUDING REMARKS

The statistical study of the spacing and the widths of the unitary collision matrix described in Secs. II and III is somewhat like the statistical study of the eigenvalues and eigenvector components of the random 2×2 real-symmetric Hamiltonian matrices, which was done by Porter and Rosenzweig[11] in the early days of the statistical model. We have shown that the spacing and the widths of the unitary collision matrix can be correlated, while the correlation between the eigenvalues and eigenvector components of the real-symmetric Hamiltonian matrices was strictly zero. We have shown how the distribution of a single width of the unitary collision matrix, depending on the ratio of the average width to average spacing of the collision matrix, differs from the usual Porter-Thomas–type distributions.

The simple model has also been used to check which of the relations between the various ensemble averages of the parameters of the statistical collision matrix, obtained using the ensemble of random complex orthogonal matrices,[3] are consistent with the constraint of unitarity.

PHYSICAL REVIEW VOLUME 173, NUMBER 4 20 SEPTEMBER 1968

Neutron Spectroscopic Factors from Isobaric Analog States*

W. J. Thompson, J. L. Adams,† and D. Robson
Department of Physics, Florida State University, Tallahassee, Florida
(Received 25 January 1968)

The spectroscopic factors S_n of bound neutron states are usually found from (d,p) stripping reactions. An alternative method of finding S_n for medium-to-heavy nuclei is to analyze isobaric analog resonances observed in (p,p) scattering from these nuclei. The present analysis uses a modified R-matrix theory in which boundary matching is done within the optical-model potential region rather than directly onto the Coulomb potential region. A resonance mixing phase and an optical penetrability are introduced. Both single- and multilevel resonances are treated. The effects of compound elastic scattering and the energy dependence of the level shift are investigated. Formulas for the spreading width are obtained. The variation of S_n with the value of the matching radius and the best choice of this radius are discussed. As examples of the method, analyses of the s-wave resonance in ^{92}Zr$(p,p)^{92}$Zr near 6.0-MeV bombarding energy and of s- and d-wave resonances in ^{90}Zr$(p,p)^{90}$Zr near 5.8 and 6.8 MeV are presented. The values of S_n obtained are compared with those from (d,p) experiments, and the reliability of the two methods is discussed.

I. INTRODUCTION

In the elastic scattering of protons from medium-to-heavy nuclei it was found that large resonance states, which are the isobaric analogs of the bound neutron-plus-target states, are produced.[1] Such resonances may be described by an R-matrix theory in which the neutron-plus-target states are simply related to the analog states formed by the proton plus target.[2]

The parameters of the analog resonances can be obtained by analyses of differential cross-section excitation functions at energies near the resonances. Corresponding polarization excitation functions also are useful in finding the best resonance parameters. An optical-model potential which describes the nonresonant (background, or $T_<$ states) scattering may be determined by fitting angular distributions taken at energies off resonance, but in the same energy region. The best situation

* Research sponsored in part by the Air Force Office of Scientific Research, Office of Aerospace Research, U. S. Air Force, under AFOSR Grant No. AF-AFOSR-440-67, and the National Science Foundation under Grant No. NSF-GP-5114.

† Present address: Ohio University, Athens, Ohio.

[1] J. D. Fox, C. F. Moore, and D. Robson, Phys. Rev. Letters 12, 198 (1964).

[2] D. Robson, Phys. Rev. 137, B535 (1965).

is to have both the resonance and off-resonance data. If compound elastic scattering is negligible, the total (p,n) cross section is essentially the same as the computed reaction cross section in many cases of interest. Thus, measurements of the (p,n) cross section are helpful in determining the absorptive part of the optical-model potential. Also, such measurements help to determine the resonance energy and total width. When data are not available off resonance, the optical-model parameters may be estimated from a standard set.[3] The resonance data are analyzed, using a modified R-matrix[4] formula. In the resonance term the effects arising from the background scattering are included. Once the proton partial width of the resonance is found, the neutron spectroscopic factor may be computed by using the relation between the neutron bound-state reduced width at the boundary matching radius and the corresponding proton reduced width for the isobaric analog state.

In Sec. II the usual R-matrix theory[4] is modified so that boundary value matching can occur inside the nuclear-interaction region. This is necessary if the region of charge independence is smaller than the region of nuclear interaction. In these applications, "charge independence" means the approximate cancellation of Coulomb effects in the internal region (Ref. 2, Fig. 1). The choice of an R-matrix formulation of the analysis is made on practical grounds, although several formally equivalent approaches are possible.[5,6] The modified R-matrix theory involves a resonance-mixing phase,[6] and an optical penetrability. It is shown that the phase $\phi_c{}^R$ is a result of the mixing between the resonances and the absorptive part of the nonresonant scattering. The estimation of this phase is discussed. The optical penetrability $P_c{}^0$ is compared with the usual Coulomb penetrability.

The formula for the elastic scattering elements of the collision matrix which include both nonresonant and resonant contributions is then derived for a single-level resonance. It is shown that the energy dependence of the level shift can be replaced by renormalization of the analog neutron wave function.

The use of a single-level formula is valid for the analysis of data which have been averaged over the fine structure in the analog resonance, and the partial width obtained is that for the averaged resonance.

For several overlapping resonances in the same channel, a multilevel formula is derived. However, the partial widths extracted are no longer simply related to the proton wave function at the boundary. Hence the extraction of spectroscopic factors is much more difficult.

Compound elastic scattering contributions arise from the energy-averaging over the fine structure, and formulas for these contributions are given in the important case of elastic scattering below reaction thresholds. In such cases, the spreading of the total width due to background scattering can also be readily calculated, as is done in Sec. II G.

In Sec. III the formula for the neutron spectroscopic factor S_n is given. The calculated values of S_n and $\phi_c{}^R$ vary with the matching radius, and methods for choosing the best radius are discussed.

Examples of the application of the theory are given in Secs. IV and V. The first is an analysis of the s-wave resonance in the elastic scattering reaction $^{92}\mathrm{Zr}(p,p)^{92}\mathrm{Zr}$ near 6.0-MeV bombarding energy. This resonance is above the (p,n) threshold, and the measured (p,n) total cross section is compared with the computed total reaction cross section. Analyses of s- and d-wave resonances near 5.8- and 6.8-MeV bombarding energies for $^{90}\mathrm{Zr}(p,p)^{90}\mathrm{Zr}$, which are presented in Sec. V, show that compound elastic scattering contributions are important below the (p,n) threshold.

The (d,p) reaction on the same target nucleus as in the proton resonance reaction preferentially populates single-partical neutron states. Neutron spectroscopic factors are usually determined from these (d,p) reactions by zero-range distorted-wave Born-approximation (DWBA) calculations.[7] A comparison of the results from the two methods is made in Sec. VI. Some of the problems encountered in both methods are also discussed.

II. ANALYSIS OF RESONANCE PLUS BACKGROUND SCATTERING

A. Boundary Matching in an Optical-Model Potential

The usual R-matrix theory of nuclear reactions[4] splits configuration space into two regions separated at a matching radius a_c, where the subscript c labels the particular channel involved. (The concept of channels is fully discussed in Ref. 4.) The purpose of this division is to have all of the unknown details of the interaction confined to the internal region $r \leq a_c$ and to have known quantities in the external region $r \geq a_c$. The interior- and exterior-region wave functions are then joined at the matching radius. The radius a_c is chosen to be large enough that the specifically nuclear interaction in the external region is negligible.[4] Then, neglecting Coulomb excitations, wave functions in different channels are orthogonal over the hypersurface containing the interior region.

For analog states it has been suggested[2] that there exists a radius inside of which the interactions are charge-independent (except for the diagonal elements of

[3] L. Rosen, J. G. Berry, A. S. Goldhaber, and E. H. Auerbach, Ann. Phys. (N. Y.) 34, 96 (1965).

[4] A. M. Lane and R. G. Thomas, Rev. Mod. Phys. 30, 257 (1958).

[5] A. M. Lane and D. Robson, Phys. Rev. 151, 774 (1966).

[6] D. Robson and A. M. Lane, Phys. Rev. 161, 982 (1967).

[7] N. Austern, in *Selected Topics in Nuclear Theory*, edited by F. Janouch (International Atomic Energy Agency, Vienna, 1963); R. H. Bassel, R. M. Drisko, and G. R. Satchler, Oak Ridge National Laboratory Report No. ORNL-3240 (unpublished).

the Coulomb interaction which are necessary to account for the observed Coulomb energy shifts). In an R-matrix theory of analog states, this would be an appropriate choice of the matching radius. If, however, the nuclear potential is not zero beyond this radius, the R-matrix requirement of channel orthogonality is no longer satisfied. If excitation effects on the elastic scattering can be represented by complex absorption terms in an optical-model potential, the stipulation that channels be orthogonal is approximately satisfied. Thus the best choice of matching radius may be complicated by the conflicting requirements that it be small enough so that charge independence holds in the internal region and yet large enough that the channels are approximately orthogonal in the external region. The advantage gained by assuming charge independence in the internal region, and using optical-model wave functions for the elastic scattering wave functions in the external region, should outweigh the error made from having channels which are only approximately orthogonal.

In order to match the interior region onto the exterior region, it is necessary to have the exterior-region wave functions which are solutions of an optical-model potential (including the Coulomb potential). Lane and Thomas (Ref. 4, Sec. VII-4) suggested the use of such optical wave functions although a detailed treatment has not been given. In the following, the notation of Lane and Thomas will be used, and corresponding equations in their Coulomb wave-function treatment will be referred to for algebraic detail. References to equations in their article will be prefixed by LT.

For the external wave functions, the regular solution $f_c(r)$ and the irregular solution $g_c(r)$ of the radial Schrödinger equation for a given optical potential and elastic channel designated c (labeled by partial wave l, channel spin, and total angular momentum j) are defined as the two linearly independent solutions with the asymptotic behavior

$$f_c(r)\sim F_l(r)\cos\delta_c+G_l(r)\sin\delta_c, \tag{1}$$

$$g_c(r)\sim -F_l(r)\sin\delta_c+G_l(r)\cos\delta_c, \tag{2}$$

where δ_c is the (complex) optical-model phase shift, and $F_l(r)$ and $G_l(r)$ are the regular and irregular Coulomb wave functions.[8] Incoming i_c and outgoing o_c solutions can be defined by

$$i_c(r)\equiv[g_c(r)-if_c(r)]\exp i\omega_l, \tag{3}$$

$$o_c(r)\equiv[g_c(r)+if_c(r)]\exp(-i\omega_l), \tag{4}$$

where ω_l is the relative Coulomb phase shift for partial wave l. From Eqs. (1) and (2), the asymptotic behavior of i_c and o_c is given by

$$i_c(r)\sim I_l(r)\exp(-i\delta_c), \tag{5}$$

$$o_c(r)\sim O_l(r)\exp i\delta_c, \tag{6}$$

where I_l and O_l are incoming and outgoing waves for the Coulomb potential [LT, Sec. III, Eq. (2.10)] so that i_c and o_c are the corresponding waves for the optical (including Coulomb) potential.

Following LT, Sec. IX-1, the R matrix is split into a background term $\mathbf{R}^0$ and resonance terms, and the elastic scattering elements of the collision matrix can be written

$$U_{cc}=U_{cc}{}^0+2i(\exp 2i\delta_c)\Omega_c{}^2\beta_c \times[(1-\mathbf{R}^0\mathbf{L}^0)^{-1}]_{cc}{}^2\sum_{\lambda\lambda'}\gamma_{\lambda c}\gamma_{\lambda' c}A_{\lambda\lambda'}(E), \tag{7}$$

where $U_{cc}{}^0$ is the background amplitude given in Eq. (22). The $\exp 2i\delta_c$ term comes about from the fact that optical, rather than Coulomb, wave functions are being used. In Eq. (7) the contributions of off-diagonal terms in $(1-\mathbf{R}^0\mathbf{L}^0)^{-1}\gamma_\lambda$ to the resonance amplitude have been neglected. The quantities Ω_c, β_c, and $\mathbf{L}^0$ are given in terms of the optical wave functions rather than the Coulomb wave functions as follows:

$$\Omega_c=(i_c/o_c)^{1/2}, \tag{8}$$

$$\beta_c=\rho_c/(i_c o_c), \tag{9}$$

$$L_c{}^0=\frac{\rho_c}{o_c}\frac{do_c}{d\rho_c}-B_c, \tag{10}$$

where

$$\rho_c=ka_c, \tag{11}$$

k is the wave number, and a_c is the matching radius. The boundary condition B_c of the elastic channel will be discussed in more detail in Sec. III. The reduced width[4] of the channel wave function is given as $\gamma_{\lambda c}$. Its relation to the partial width $\Gamma_{\lambda\lambda,c}$ will be considered shortly. The $A_{\lambda\lambda'}(E)$ are elements of the level matrix[4]

$$(\mathbf{A}^{-1})_{\lambda\lambda'}=(E_\lambda-E)\delta_{\lambda\lambda'}+\Delta_{\lambda\lambda'}-\tfrac{1}{2}i\Gamma_{\lambda\lambda'}. \tag{12}$$

The shift ($\mathbf{\Delta}$) and width ($\mathbf{\Gamma}$) matrices are given by the relation

$$-\Delta_{\lambda\lambda'}+\tfrac{1}{2}i\Gamma_{\lambda\lambda'}=\sum\gamma_{\lambda c}\gamma_{\lambda' c}L_c{}^0[(1-\mathbf{R}^0\mathbf{L}^0)^{-1}]_{cc}, \tag{13}$$

the summation over channels including all those with nonzero values of $L_c{}^0\gamma_{\lambda c}\gamma_{\lambda' c}$. The matrices $\mathbf{\Delta}$ and $\mathbf{\Gamma}$ are usually assumed to be energy-independent.

In previous analyses[9] the term dividing the reduced width has been neglected or only estimated, Ω_c and β_c were replaced by their values for the Coulomb wave functions, and δ_c was set at zero. The expression dividing the reduced width can be written as

$$[(1-\mathbf{R}^0\mathbf{L}^0)^{-1}]_{cc}=(1-R_{cc}{}^{\mathrm{opt}}L_c{}^0)^{-1}, \tag{14}$$

and $R_{cc}{}^{\mathrm{opt}}$ is approximated as [see LT, Sec. IV, Eq. (2.4)]

$$R_{cc}{}^{\mathrm{opt}}=\left(\frac{\rho_c}{f_c}\cdot\frac{df_c}{d\rho_c}-B_c\right)^{-1}. \tag{15}$$

[8] M. H. Hull and G. Breit, in *Handbuch der Physik*, edited by S. Flügge (Springer-Verlag, Berlin, 1959), Vol. XLI/I, p. 408.

[9] P. von Brentano, in *Proceedings of the Conference on Isobaric Spin in Nuclear Physics*, edited by J. D. Fox and D. Robson (Academic Press Inc., New York, 1966), paper C2.

Equation (14) arises when the collision amplitude is averaged over a small energy interval F such that the fine structure is smoothed out. This procedure corresponds to replacing $U_{cc}(E)$ by $U_{cc}(E+iF)$ which is here denoted by $\langle U_{cc}\rangle$. If Eqs. (8)–(14) are inserted into expression (7) for U_{cc}, the following is obtained:

$$\langle U_{cc}\rangle=\langle U_{cc}{}^0\rangle+i\exp[2i(\delta_c+\omega_l)]\times\exp(2i\phi_c{}^R)2P_c{}^0\sum_{\lambda\lambda'}\gamma_{\lambda c}\gamma_{\lambda' c}A_{\lambda\lambda'}(E). \quad (16)$$

Here the optical penetrability $P_c{}^0$ is defined by

$$P_c{}^0=\rho_c(d_R{}^2+d_I{}^2), \quad (17)$$

where d_R and d_I are given by

$$d_R=\mathrm{Re}[(df_c/d\rho)_{r=a_c}-f_cb_c], \quad (18)$$

$$d_I=\mathrm{Im}[(df_c/d\rho)_{r=a_c}-f_cb_c], \quad (19)$$

where

$$b_c=B_c/\rho_c. \quad (20)$$

The resonance mixing phase $\phi_c{}^R$ is defined by

$$\phi_c{}^R=\tfrac{1}{2}\tan^{-1}(d_I/d_R). \quad (21)$$

Note that the irregular solution g_c [Eq. (2)] does not appear in the final formulas for $P_c{}^0$ and $\phi_c{}^R$.

The background scattering collision amplitude may be written

$$\langle U_{cc}{}^0\rangle=\exp[2i(\delta_c+\omega_l)], \quad (22)$$

and

$$\delta_c=\xi_c+i\zeta_c, \quad (23)$$

where both ξ_c and ζ_c are real. The phase shift δ_c is usually approximated by an optical-model phase shift. Equation (16) can then be written

$$\langle U_{cc}\rangle=\langle U_{cc}{}^0\rangle+i\exp[2i(\xi_c+\omega_l+\phi_c{}^R)]\times\sum_{\lambda\lambda'}(\Gamma_{\lambda\lambda,c}\Gamma_{\lambda'\lambda',c})^{1/2}A_{\lambda\lambda'}(E), \quad (24)$$

where the partial width $\Gamma_{\lambda\lambda,c}$, which determines the magnitude of the resonance amplitude, is

$$\Gamma_{\lambda\lambda,c}=2P_c{}^0\exp(-2\zeta_c)\gamma_{\lambda c}{}^2. \quad (25)$$

The relations between the differential cross section, the polarization in the Basel convention, and the scattering of a spin-$\frac{1}{2}$ projectile from a spin-0 target are given by

$$\frac{d\sigma}{d\Omega}=|a|^2+|b|^2, \quad (26)$$

$$P(\theta)=2\,\mathrm{Im}(ab^*)(|a|^2+|b|^2)^{-1}, \quad (27)$$

where

$$a(\theta)=-\eta\exp\{-i\eta\ln[\sin^2(\tfrac{1}{2}\theta)]\}[2k\sin^2(\tfrac{1}{2}\theta)]^{-1}+\frac{1}{2ik}\sum_{l,j}(j+\tfrac{1}{2})(U_{cc}-\exp2i\omega_l)P_l(\cos\theta), \quad (28)$$

$$b(\theta)=\frac{1}{2ik}\sum_{l,j}(-1)^{j-l-1/2}(U_{cc}-\exp2i\omega_l)P_l{}^1(\cos\theta). \quad (29)$$

In the above equations, θ is the scattering angle in the center-of-mass system, η is the Coulomb parameter, and k is the wave number. The channel c is labeled by l and j.

B. Resonance-Mixing Phase

The resonance-mixing phase $\phi_c{}^R$, defined by Eq. (21), vanishes for a real background potential for which the wave function f_c [Eq. (1)] is real. Thus $\phi_c{}^R$ arises from the effect of the absorptive parts of the background scattering on the phase of the resonance scattering. Therefore $\phi_c{}^R$ is expected to increase with the absorptive terms in the optical-model potential. For large a_c, $\phi_c{}^R$ depends on $\tanh\zeta_c$,

$$\tan2\phi_c{}^R\sim(\tanh\zeta_c)/\tan(\varphi_c+\xi_c), \quad (30)$$

where

$$\tan\varphi_c=(F_l'-F_lb_c)/(G_l'-G_lb_c). \quad (31)$$

Since f_c is only weakly energy-dependent, and b_c is constant, $\phi_c{}^R$ may be taken as a constant across any group of closely spaced resonances belonging to channel c, since it is also independent of λ.

The phase $\phi_c{}^R$ is also limited by unitarity, $|U_{cc}|\leq1$. For a single-level resonance (Sec. II D),

$$\cos\{2\phi_c{}^R+\tan^{-1}[2(E_R-E)/\Gamma_{\lambda\lambda}]\}\geqslant\frac{1}{2}\left[\exp(-2\zeta_c)-\left(1-\frac{\Gamma_{\lambda\lambda,c}{}^2}{(E_R-E)^2+(\Gamma_{\lambda\lambda}/2)^2}\right)\exp2\zeta_c\right], \quad (32)$$

together with the restriction on the background absorption

$$\exp(-2\zeta_c)\geqslant\left[2-\left(\frac{2\Gamma_{\lambda\lambda,c}}{\Gamma_{\lambda\lambda}}\right)^2\right]^{1/2}-1. \quad (33)$$

The unitarity condition Eq. (32) is thus energy-dependent.

In previous analyses of resonances $\phi_c{}^R$ has usually been set to zero. For a single-level resonance, such an analysis would shift the resonance energy to roughly $\Gamma_{\lambda\lambda}\phi_c{}^R$ ($\phi_c{}^R$ in radians) below the resonance energy determined when $\phi_c{}^R$ is taken into account. ($\Gamma_{\lambda\lambda}$ is the total width of the resonance.) This displacement is typically about 10 keV. An example of the effect of $\phi_c{}^R$ on the shape of the excitation function is given in Fig. 2, and the dependence of $\phi_c{}^R$ on the matching radius is shown in Figs. 4, 9, and 10.

Previous work (Ref. 10, Fig. 8) has shown that the elastic scattering polarization should be sensitive to $\phi_c{}^R$.

C. Optical Penetrability

The optical penetrability $P_c{}^0$ defined in Eq. (17), depends both on the optical-model wave functions $f_c(r)$ and on the choice of boundary conditions b_c. As is seen from Eq. (25), the effective penetrability, relating the

[10] J. L. Adams, W. J. Thompson, and D. Robson, Nucl. Phys. 89, 377 (1966).

observed partial width to the reduced width, is

$$P_c^{\rm opt}=P_c^0\exp(-2\zeta_c). \quad (34)$$

The Coulomb penetrability P_c is usually employed in Eq. (25). The quantity P_c is defined in terms of the Coulomb wave functions by[4]

$$P_c=\rho_c/[F_l^2(a_c)+G_l^2(a_c)]. \quad (35)$$

The reduced width $\gamma_{\lambda c}^2$ can usually be directly related to nuclear-structure calculations, but accurate determination of $\gamma_{\lambda c}^2$ from experimental data requires accurate values of the penetrability. Moreover, the radius chosen for the estimation of $\gamma_{\lambda c}^2$ is often small enough that the nuclear potential is still significant. Then $P_c^{\rm opt}$ rather than P_c should be used to obtain $\gamma_{\lambda c}^2$ from $\Gamma_{\lambda\lambda,c}$.

Comparisons of the effective penetrability in the optical-model potential $P_c^{\rm opt}$, with the Coulomb penetrability P_c, show that for protons the two quantities often differ by $\pm 30\%$, and cannot be brought into agreement merely by using the reflection coefficient $\exp(-2\zeta_c)$. It is therefore important for the accurate estimation of reduced widths using R-matrix theory that Eq. (34) rather than Eq. (35) be used even if the matching radius is beyond the nuclear potential. The dependence of the penetrabilities $P_c^{\rm opt}$ and P_c on the matching radius a_c can be compared in Figs. 4, 9, and 10.

D. Single-Level Resonance with Level Shift

For a single isolated resonance level, Eq. (12) gives

$$A_{\lambda\lambda}=[E_\lambda+\Delta_{\lambda\lambda}(E)-E-\tfrac{1}{2}i\Gamma_{\lambda\lambda}]^{-1}. \quad (36)$$

At the resonance energy E_R,

$$E_\lambda+\Delta_{\lambda\lambda}(E_R)-E_R=0. \quad (37)$$

The energy dependence of the level shift $\Delta_{\lambda\lambda}$ is usually ignored, but it can be treated approximately as follows: An expansion of the level shift $\Delta_{\lambda\lambda}$ in a Taylor series about E_R gives, to first order (which is sufficiently accurate away from thresholds),

$$E_\lambda+\Delta_{\lambda\lambda}(E)-E=(E_R-E)[1-(\partial\Delta_{\lambda\lambda}/\partial E)_{E=E_R}]. \quad (38)$$

It can be shown (Ref. 4, p. 351) that, neglecting the background terms in Eq. (13), the effect of the first-order energy dependence of the shift corresponds to taking the normalization of bound states to unity over all space, rather than to unity within the internal region, i.e.,

$$\left[1-\left(\frac{\partial\Delta_{\lambda\lambda}}{\partial E}\right)_{E=E_R}\right]=1+\int_{a_c}^{\infty}|\Psi|^2d\tau,$$

with

$$\int_0^{a_c}|\Psi|^2d\tau=1$$

defining the normalization of the total wave function Ψ.

If the energy dependence of the total width $\Gamma_{\lambda\lambda}$ is negligible, as will often be the case, then for a single isolated resonance level

$$\langle U_{cc}\rangle=\langle U_{cc}^0\rangle+i\exp[2i(\xi_c+\omega_l+\phi_c^R)]\times\Gamma_{\lambda c}/(E_R-E-\tfrac{1}{2}i\Gamma_\lambda), \quad (39)$$

where

$$\Gamma_\lambda=[1-(\partial\Delta_{\lambda\lambda}/\partial E)_{E=E_R}]^{-1}\Gamma_{\lambda\lambda},$$
$$\Gamma_{\lambda c}=2P_c^{\rm opt}(\gamma_{\lambda c}')^2, \quad (40)$$
$$\gamma_{\lambda c}'=[1-(\partial\Delta_{\lambda\lambda}/\partial E)_{E=E_R}]^{-1/2}\gamma_{\lambda c}.$$

All of the formulas in earlier sections should be modified according to Eqs. (39) and (40), although ratios of widths are of course unaltered.

Equations (39) and (40) are appropriate for isobaric analog resonances since the (bound) charge-exchange neutron channels dominate $\partial\Delta_{\lambda\lambda}/\partial E$ to order $(N+1-Z)^{-1}$. Hence the effect of the first-order energy dependence of the shift corresponds to the use of a wave function with a normalization region which extends to infinity in the radial separation in all closed channels.

The normalization of the bound-state wave functions is now the same for both the R-matrix analysis of single-level (p,p) analog resonances and the DWBA analysis of (d,p) stripping reactions. Hence the values of the neutron spectroscopic factors obtained from the two methods may be directly compared.

In Eq. (39) the second term is the resonance term, and there can only be one such term for each spin and parity (J^π). (For elastic scattering of a spin-$\frac{1}{2}$ projectile from a spin-0 target there is only one elastic channel c for each value of J^π.) However, the differential cross section and polarization result from contributions of several U_{cc}, each of which can have at most one resonance. Thus the cross section and polarization may be analyzed with such a "many-level" formula even if several resonances overlap, as long as no two overlapping resonances have the same J^π. For two or more overlapping resonances with the same J^π a multilevel resonance formula, described in Sec. II E, must be used.

E. Multilevel Resonance Formulas

In the situation where resonances with the same J^π are close together, the multilevel resonance formula given by Eq. (16) must be used. The two- and three-level formulas are given in Ref. 4, Sec. IX-1(b), and give the energy dependence of the resonance amplitude explicitly.

An alternative form of Eq. (16) which is somewhat simpler is obtained by use of a complex orthogonal transformation T, which diagonalizes the level matrix

$$\mathbf{T}\mathbf{A}^{-1}\tilde{\mathbf{T}}=\mathbf{F}-\mathbf{E}-\tfrac{1}{2}i\boldsymbol{\Gamma}'. \quad (41)$$

The collision-matrix elastic scattering elements take the form

$$\langle U_{cc}\rangle=\langle U_{cc}^0\rangle+i\exp[2i(\xi_c+\omega_l+\phi_c^R)]\times\sum_\mu\frac{g_{\mu c}^2}{(F_\mu-E-\tfrac{1}{2}i\Gamma_\mu')}, \quad (42)$$

with

$$g_{\mu c}^2=2P_c^0\exp(-2\zeta_c)\theta_{\mu c}^2, \quad (43)$$

where

$$\theta_{\mu c}=\sum_\lambda T_{\mu\lambda}\gamma_{\lambda c}. \quad (44)$$

The advantage of Eq. (42) over Eq. (16) is that it usually involves fewer parameters to describe the elastic scattering resonances. Note that this may not be the case when one attempts to analyze overlapping levels in all open channels. The restriction to elastic scattering analyses makes Eq. (42) attractive in the present work.

An empirical analysis for N overlapping levels using Eq. (16) requires $N(N+2)$ real parameters to describe the elastic resonances, whereas Eq. (42) needs only $4N$ real parameters. For $N=2$, both methods involve eight real parameters, but for $N\geq 3$, Eq. (42) involves considerably fewer parameters than Eq. (16), and is therefore to be preferred in such cases. Even for $N=2$, Eq. (42) is simpler computationally. The disadvantage of Eq. (42), however, is that "reduced widths" $\theta_{\mu c}^2$ are not easily related to the conventional neutron reduced widths which are to be extracted. Moreover, the resonance parameters in Eq. (42) could be strongly energy-dependent. In the case $N=2$, therefore, it may be more convenient to use Eq. (16) for the empirical analysis. Some efforts to analyze data via Eq. (42) are being made elsewhere.[11]

For isobaric analog states the coefficients $T_{\mu\lambda}$ arise from the admixtures of analog states amongst themselves due to the Coulomb mixing from boundary-condition changes alone, assuming charge independence in the internal region. It is questionable whether Coulomb mixing between analog states from the internal region can be neglected, even though it appears a reasonable approximation to neglect internal mixing between states of different isobaric spin. It is not hard to formally include internal mixing between analog states; the only change is that the matrix $\mathbf{A}^{-1}$ is replaced by the matrix $\mathbf{B}^{-1}$, where $\mathbf{B}^{-1}$ has elements

$$(\mathbf{B}^{-1})_{\lambda\lambda'}=(E_\lambda-E)\delta_{\lambda\lambda'}+\Delta_{\lambda\lambda'}-\tfrac{1}{2}i\Gamma_{\lambda\lambda'}+H'_{\lambda\lambda'}, \quad (45)$$

where $\mathbf{H}'$ is the internal Coulomb mixing operator as discussed by Robson and Lane.[6] The matrix $\mathbf{F}-\mathbf{E}-\frac{1}{2}i\boldsymbol{\Gamma}'$ is then obtained from $\mathbf{TB}^{-1},\tilde{\mathbf{T}}$ so that the coefficients $T_{\mu\lambda}$ in Eq. (44) still play the role of describing dynamic distortion between analog states, as discussed by MacDonald,[12] and Eqs. (16) and (42) remain valid with $\mathbf{A}$ replaced by $\mathbf{B}$.

F. Compound Elastic Scattering

The requirements for a single isolated resonance level can seldom be met except for very light nuclei. The exact treatment of multilevel formulas becomes intractable when the ratio of level widths to level spacing becomes large, as is the case for high excitation of the compound nucleus formed in elastic scattering through isobaric analog states. However, in most experiments the energy spread of the incident projectiles is much greater than the level spacing, so that the observed cross section is an energy average over many levels in the compound nucleus. In the analysis of isobaric analog states with a few-level resonance formula, the scattering matrix used is an energy-averaged matrix. Therefore, allowance must be made for the effects on the average cross section of using an averaged scattering matrix.

The elastic scattering differential cross section for a spin-0 target and a spin-$\frac{1}{2}$ projectile can be conveniently written for the present purpose[4]:

$$\frac{d\sigma}{d\Omega}=\left(\frac{d\sigma}{d\Omega}\right)_{\text{Coul}}+\frac{1}{2k^2}\sum_L B_L P_L(\cos\theta) + (\text{interference terms}), \quad (46)$$

where $(d\sigma/d\Omega)_{\text{Coul}}$ is the scattering cross section for the Coulomb potential, k is the wave number of the relative motion, and B_L is given by

$$B_L=\tfrac{1}{4}\sum_{cc'}\bar{Z}^2(ljl'j',\tfrac{1}{2}L)T_cT_{c'}^*, \quad (47)$$

with

$$\bar{Z}(ljl'j',sL)=[(2l+1)(2l'+1)(2j+1)(2j'+1)]^{1/2}\times(ll'00|L0)W(ljl'j';sL) \quad (48)$$

and

$$T_c=(\exp 2i\omega_l)-U_{cc}. \quad (49)$$

In the above equation $c=(l,j)$ and $c'=(l',j')$. In Eq. (48) appear the Clebsch-Gordan coefficient and Racah's W coefficient.

The measured energy-averaged differential cross section $\langle d\sigma/d\Omega\rangle$ is obtained by averaging Eq. (46). It can be written

$$\left\langle\frac{d\sigma}{d\Omega}\right\rangle=\left(\frac{d\sigma}{d\Omega}\right)_{\text{DI}}+\left(\frac{d\sigma}{d\Omega}\right)_{\text{CE}}. \quad (50)$$

The direct-interaction elastic cross section is defined to be that obtained by using the matrix elements $\langle U_{cc}\rangle$ of Eq. (24) as the energy-averaged matrix elements $\langle U_{cc}\rangle$, with a background matrix $\langle U_{cc}^0\rangle$ from the optical model, and a few-level formula for the resonance terms. The energy-averaged compound elastic cross section $(d\sigma/d\Omega)_{\text{CE}}$ is then readily obtained from Eqs. (46) and (50). The result is

$$\left(\frac{d\sigma}{d\Omega}\right)_{\text{CE}}=\frac{1}{8k^2}\sum_{cc'}\bar{Z}^2(ljl'j',\tfrac{1}{2}L)T_{cc'}P_L(\cos\theta), \quad (51)$$

where

$$T_{cc'}=\langle U_{cc}U_{c'c'}^*\rangle-\langle U_{cc}\rangle\langle U_{c'c'}^*\rangle. \quad (52)$$

[11] G. Temmer (private communication); L. Veeser (private communication).

[12] W. M. MacDonald, in *Nuclear Spectroscopy*, edited by F. Ajzenberg-Selove (Academic Press Inc., New York, 1960), Part B, p. 932.

Since isobaric analog resonances with protons are often observed below the Coulomb barrier, the reaction channels are dominated by neutron emission for proton bombarding energies above the (p,n) threshold. However, then the compound elastic scattering itself usually becomes negligible. This will be discussed further in Sec. IV.

If only the elastic scattering channels are open, as is often a good approximation below the (p,n) threshold, the (unaveraged) scattering matrix is diagonal, so that

$$\left(\frac{d\sigma}{d\Omega}\right)_{\mathrm{CE}}=\frac{1}{8k^2}\sum_c \bar{Z}^2(ljlj,\tfrac{1}{2}L) \times(1-|\langle U_{cc}\rangle|^2)P_L(\cos\theta). \quad (53)$$

That is, T_{cc} of Eq. (52) is just the transmission coefficient

$$T_{cc}=1-|\langle U_{cc}\rangle|^2, \quad (54)$$

where $\langle U_{cc}\rangle$ is given by the right-hand side of Eq. (24).

If a single-level resonance dominates the elastic scattering and if background scattering is ignored, then a simple example of compound elastic scattering is obtained. For then Eq. (39) has $\langle U_{cc}{}^0\rangle=\exp 2i\omega_l$ and $\xi_c=\phi_c{}^R=0$, so that

$$T_{cc}=\frac{\Gamma_{\lambda c}(\Gamma_\lambda-\Gamma_{\lambda c})}{(E_R-E)^2+(\frac{1}{2}\Gamma_\lambda)^2}. \quad (55)$$

The term $\Gamma_\lambda-\Gamma_{\lambda c}$ can be interpreted as the partial width for the decay back into the elastic channel through the compound nucleus. However, absorption, and thus compound elastic scattering, is also important for the background terms. This is illustrated in Fig. 6 for $^{93}\mathrm{Zr}(p,p)^{90}\mathrm{Zr}$ at an off-resonance energy below the (p,n) threshold. When the resonance mixing phase $\phi_c{}^R$ is nonzero the transmission coefficient is asymmetric about the resonance energy, as discussed in more detail by Robson and Lane.[6]

From Eqs. (48) and (51) it follows that the compound elastic contribution is symmetric about 90°. Each channel contributes even at angles where the corresponding direct contribution vanishes, as at the zeros of $P_l(\cos\theta)$. An example is shown in Fig. 7 for a d-wave resonance excitation function at 125°measured near 6.8 MeV.

The angle-integrated compound elastic cross section below thresholds is equal to the total reaction cross section defined by Eq. (70).

The measured energy-averaged polarization is

$$P_m=\left\langle\frac{d\sigma}{d\Omega}P\right\rangle\Big/\left\langle\frac{d\sigma}{d\Omega}\right\rangle, \quad (56)$$

where P is the polarization at each energy. It is readily shown[13] that if the compound-nucleus reduced widths have random signs, or if only elastic scattering channels are open, then $\langle(d\sigma/d\Omega)P\rangle$ has no compound-nucleus contributions. Therefore, it may be calculated from the $\langle U_{cc}\rangle$ given by Eq. (24). However, as discussed above, $\langle d\sigma/d\Omega\rangle$ may have large compound-nucleus contributions; then so has P_m. In such cases P_m may be much different from the polarization P calculated using Eq. (27) at the average energy. Note also that $|P_m|\leq P$. In Fig. 8 a comparison of P_m and P is made for the polarization excitation function near the 6.8-MeV resonance in $^{90}\mathrm{Zr}(p,p)^{90}\mathrm{Zr}$. It is seen, as expected, that P_m (solid line) gives a better fit to the data than does P (dashed line).

[13] W. J. Thompson, Phys. Letters **25B**, 454 (1967).

G. Spreading Width

An interpretation, alternative to that made from Eq. (55), of the spreading of the observed total width Γ_λ from the observed partial width $\Gamma_{\lambda c}$ can be made. Define the spreading width in channel c, $W_{\lambda c}$, by

$$\Gamma_\lambda=\sum_c(\Gamma_{\lambda c}+W_{\lambda c}), \quad (57)$$

where the sum over c includes only isobaric-spin-allowed channels. Above thresholds $W_{\lambda c}$ is nonzero because of the decay widths into other open channels. The widths are often difficult to measure or calculate. However, when only elastic scattering is significant $W_{\lambda c}$ is still nonzero because of absorptive terms in the background scattering (or, in isobaric-analog language, by external mixing with $T_<$ states). An elastic channel c contributes to the total width, by Eqs. (13) and (14),

$$\Gamma_{\lambda\lambda,c}+W_{\lambda\lambda,c}=2\,\mathrm{Im}[L_c{}^0(1-R_{cc}{}^{\mathrm{opt}}L_c{}^0)^{-1}]\gamma_{\lambda c}{}^2, \quad (58)$$

where

$$\Gamma_{\lambda\lambda}=\sum_c(\Gamma_{\lambda\lambda,c}+W_{\lambda\lambda,c})=\left[1-\left(\frac{\partial\Delta_{\lambda\lambda}}{\partial E}\right)_{E=E_R}\right]\Gamma_\lambda. \quad (59)$$

The ratio $W_{\lambda c}/\Gamma_{\lambda c}=W_{\lambda\lambda,c}/\Gamma_{\lambda\lambda,c}$ is independent of the choice of wave-function normalization, which affects only the reduced widths, so that formulas without the energy shift correction (Sec. II D) may be used. Some manipulation then gives, for the elastic-channel contribution to the spreading width, the calculated value

$$\left(\frac{W_{\lambda c}}{\Gamma_{\lambda c}}\right)_{\mathrm{calc}}=\exp 2\zeta_c\,\mathrm{Im}\left[\exp 2i\phi_c{}^R\left(\frac{g_c{}'-b_cg_c}{f_c{}'-b_cf_c}+i\right)\right]-1. \quad (60)$$

When the optical-model potential, which describes the background scattering, is real, f_c and g_c are real, and ζ_c and $\phi_c{}^R$ are zero. Hence, since the boundary condition b_c is real, the elastic-channel spreading width $W_{\lambda c}$ is zero when there are no absorptive terms in the background scattering.

Comparison of the value of the spreading width obtained from the fitted resonance parameters Γ_λ and $\Gamma_{\lambda c}$ with the values calculated from Eq. (60) can be made;

$$(\Gamma_\lambda/\Gamma_{\lambda c}-1)_{\mathrm{expt}}\approx W_{\lambda c}/\Gamma_{\lambda c}, \quad (61)$$

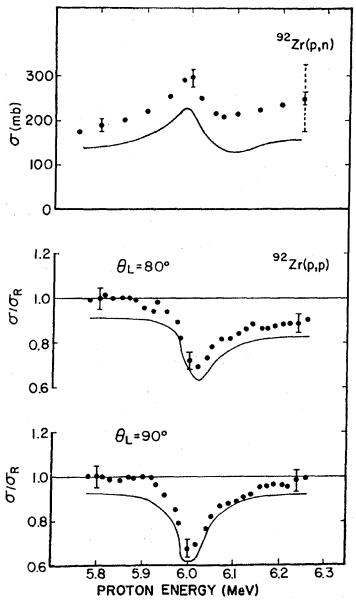

FIG. 1. Excitation function for $^{92}Zr(p,n)^{92}Nb$ total cross section. Relative errors are 5%, normalization error (shown dashed) 30%. Excitation function for $^{92}Zr(p,p)^{92}Zr$ at 80° and 90°, plotted as ratio-to-Rutherford. Absolute errors are 5%. Curves use parameters in Table I.

provided that the inelastic reduced widths are negligible, and internal-mixing effects are ignored. Such comparisons are shown in Figs. 4, 9, and 10.

In concluding Sec. II it should be noted that most of the equations thus far derived are not restricted to isobaric analog resonances. The formulas depend on the assumptions that $R_{cc}^{\rm opt}$ is well approximated as given in Eq. (13), that a diagonal background plus resonance term is a good description of the elastic scattering, and that the matching radius chosen is large enough so that the channel-orthogonality requirement is approximately satisfied. The use of the modified R-matrix treatment given here should therefore lead to more accurate estimates of nuclear-resonance parameters than have been previously obtained.

III. NEUTRON SPECTROSCOPIC FACTORS

Because of the assumption of charge independence in the interior region, the logarithmic derivative of the proton wave function of the analog state at the matching radius should be the same as that for the parent analog state neutron wave function if the boundary conditions are suitably chosen.[2] Thus, the b_c of Eq. (20) is chosen as

$$b_c=\left(\frac{1}{u_n}\frac{du_n}{d\rho}\right)_{r=a_c}. \tag{62}$$

Here u_n is the bound-state neutron radial wave function. It may be conveniently calculated by solving the radial wave equation for a neutron in a central potential $V_n(r)$ (which may depend on l_n and j_n through a spin-orbit term):

$$\frac{d^2u_n(r)}{dr^2}-\left(\frac{2m}{\hbar^2}[\epsilon_n+V_n(r)]+\frac{l_n(l_n+1)}{r^2}\right)u_n(r)=0. \tag{63}$$

Here ϵ_n is the (positive) neutron binding energy, m is the reduced mass of the neutron and target, and l_n and j_n are the orbital and total angular momentum quantum numbers of the neutron in the potential $V_n(r)$. These quantum numbers are the same as those for the proton resonance.

The neutron single-particle spectroscopic factor S_n, for a given nuclear state (λ) and channel c, is now defined as the ratio of the actual neutron probability density in channel c integrated over the surface at the matching radius a_c to the corresponding quantity for a single-particle neutron state in the same (bound) channel. It is also required that the neutron wave functions in different channels be orthogonal. Thus,

$$S_n=[\gamma_{\lambda n}'(a_c)]^2/\gamma_n^2(a_c), \tag{64}$$

where

$$\gamma_n^2(a_c)=(\hbar^2/2ma_c)u_n^2(a_c), \tag{65}$$

and $u_n^2(r)$ is normalized to unit integral over all space, as discussed in Sec. II D, i.e.,

$$\int_0^\infty u_n^2(r)dr=1. \tag{66}$$

It should be emphasized that $(\gamma_{\lambda n}')^2$ is the "observed" reduced width [cf. Eq. (40)] and also corresponds to a wave function normalized to unity over all space.

According to the theory of isobaric analog resonance states,[2] if nuclear forces are charge-independent in the interior region, the ratio of the neutron reduced width for a state λ to the reduced width for the proton analog state in the channel with the same angular momentum quantum numbers is given by

$$\gamma_{\lambda n}^2(a_c)/\gamma_{\lambda c}^2(a_c)=N+1-Z, \tag{67}$$

and to order $(N+1-Z)^{-1}$

$$[\gamma_{\lambda n}'(a_c)]^2/[\gamma_{\lambda c}'(a_c)]^2=N+1-Z. \tag{68}$$

Equation (68) would follow exactly from Eq. (67) if the proton and neutron shift functions had the same energy derivatives. Here N and Z are the neutron and proton numbers of the target nucleus. The ratio of neutron-to-proton reduced widths is just the neutron excess in the parent analog state. Combining Eqs. (25), (40), (64), and (68) gives

$$S_n=(N+1-Z)\Gamma_{\lambda c}/[2P_c^{\rm opt}\gamma_n^2(a_c)]. \tag{69}$$

If the partial width of the proton resonance $\Gamma_{\lambda c}$ has been determined from an experimental analysis, the spectroscopic factor can be computed using Eq. (69). The actual spectroscopic factor should be independent of the radius a_c. However, the value of S_n computed from Eq. (69) will be dependent on the radius, since

Eq. (67) may be true only for a particular a_c. Thus a decision as how to best choose the radius must be made. The region of charge independence is believed to extend to about the nuclear surface. Thus by examining the radial dependence of S_n near the nuclear radius (e.g., $r_0A^{1/3}$), an idea as to the best values of S_n and a_c may be obtained. If S_n is found to be approximately constant over much of this region, the choice of a_c will have little effect and a good estimate of S_n can be made. Another possibility is that S_n will go through a minimum. If this occurs, the best value of the matching radius may be chosen to be the one where S_n has its minimum value, since at this radius S_n is most nearly a constant. If neither of the above-mentioned cases held, the calculation of S_n would be unreliable.

For any choice of radius, a calculation of the resonance mixing phase $\phi_c{}^R$ can be made from Eq. (21). If $\phi_c{}^R$ is very radius-dependent, its correct value will be uncertain. However, $\phi_c{}^R$ can also be determined by an analysis of the experimental data, since it is a fitting parameter for differential cross-section and polarization data near a resonance. Very good experimental data and careful analyses are needed to determine the best value for $\phi_c{}^R$. In previous analyses, $\phi_c{}^R$ has been ignored. Examples of the dependence of S_n and $\phi_c{}^R$ on the matching radius a_c are given in Figs. 4, 9, and 10.

IV. ANALYSIS OF ^{92}Zr$(p,p)^{92}$Zr AND ^{92}Zr$(p,n)^{92}$Nb

A. Optical-Model and Single-Level Resonance Parameters

The computer code ANSPEC[14] was written to analyze isobaric analog single-level resonances in proton elastic scattering from spin-0 nuclei, including finite-target energy-loss effects.

Data at laboratory angles θ_L of 80°, 90°, 100°, 110°, 125°, 137.5°, 150°, and 165° were available for ^{92}Zr$(p,p)^{92}$Zr differential cross-section excitation functions near the laboratory resonance energy of 6.00 MeV. These data, shown in Figs. 1–3 plotted as ratio-to-Rutherford, have over-all errors of about 5%. The parent analog state of this resonance is the 0.96-MeV $\frac{1}{2}^+$ level in ^{93}Zr.[15]

In addition, the total cross section of the ^{92}Zr$(p,n)^{92}$Nb reaction had been measured near this energy using the same target.[16] The ^{92}Zr$(p,n)^{92}$Nb data were also analyzed because they were sensitive to the optical-model and resonance parameters. However the absolute error in the (p,n) cross section was 30%.[16] At 6-MeV proton energy the inelastic scattering cross section should be much less than the (p,n) cross section of about 200 mb, since the Coulomb penetrability in the inelastic proton channel is less than 1% of the neutron penetrability. Compound elastic scattering is also small (see below). It was assumed, therefore, that the total (p,n) cross section approximated the total reaction cross section (σ_r) as computed from the optical model. For a spin-0 target nucleus σ_r is

$$\sigma_r=\frac{\pi}{2k^2}\sum_{lj}(2j+1)[1-|\langle U_{lj,lj}\rangle|^2], \qquad (70)$$

where $\langle U_{lj,lj}\rangle$ is given by Eq. (24). This quantity is calculated in ANSPEC.

Previous analysis[16] of the (p,p) excitation functions at 125° and 165° allowed an arbitrary angle-dependent normalization between yield and cross section. In the present analysis, data were normalized by elastic scattering measurements at 4 MeV, where the cross section is Rutherford to within 2%. A systematic error in the normalization procedure does not affect the relative cross sections between different angles.

Preliminary fits to the (p,p) and (p,n) data using previously extracted resonance parameters from the (p,p) data,[16] and the optical-model parameters of Rosen *et al.*[3] gave poor results. However, good fits to the eight (p,p) differential cross-section excitation functions could be obtained with the resonance and optical-model parameters given in Table I. The optical-model potential used was

$$V(r)=-(V+iW)f(r)-iW'g(r)$$
$$-V_{so}h(r)\boldsymbol{\sigma}\cdot\mathbf{l}+V_C(r), \qquad (71)$$

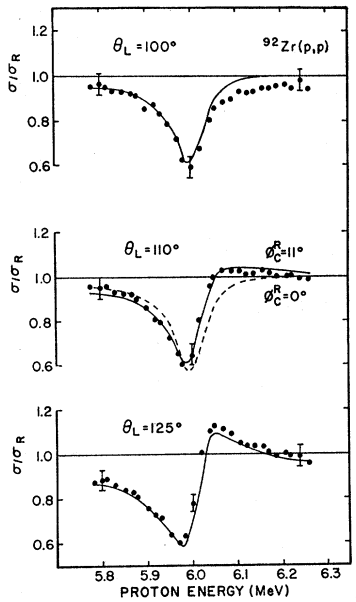

FIG. 2. Excitation function for ^{92}Zr$(p,p)^{92}$Zr at 100°, 110°, and 125°, plotted as ratio-to-Rutherford. Absolute errors are 5%. Curves use parameters in Table I. Dashed curve is for $\phi_c{}^R=0°$.

[14] W. J. Thompson and J. L. Adams, Tandem Accelerator Laboratory, Florida State University, Technical Report No. 10, 1967 (unpublished).

[15] B. L. Cohen and O. V. Chubinsky, Phys. Rev. **131**, 2184 (1963).

[16] D. Robson, J. D. Fox, P. Richard, and C. F. Moore, Phys. Letters **18**, 86 (1965).

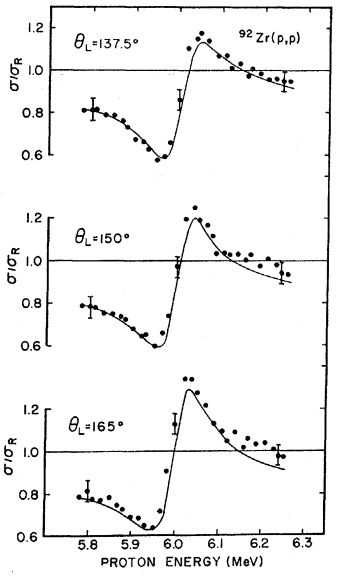

FIG. 3. Excitation function for ^{92}Zr$(p,p)^{92}$Zr at 137.5°, 150°, and 165°, plotted as ratio-to-Rutherford. Absolute errors are 5%. Curves use parameters in Table I.

where

$$f(r)=\left[1+\exp\left(\frac{r-R}{a}\right)\right]^{-1}, \tag{72}$$

$$g(r)=4\exp\left(\frac{r-R}{a'}\right)\left[1+\exp\left(\frac{r-R}{a'}\right)\right]^{-2}, \tag{73}$$

$$h(r)=-\frac{2}{r}\frac{df(r)}{dr}, \tag{74}$$

$$V_C(r)=\frac{Z_pZ_Te^2}{2R}\left[3-\left(\frac{r}{R}\right)^2\right], \quad r\leqslant R \tag{75}$$

$$=Z_pZ_Te^2/r, \qquad r\geqslant R,$$

$$R=r_0A^{1/3}, \tag{76}$$

where Z_p and Z_T are projectile and target charge numbers, and A is the atomic number of the target. The single-level resonance parameters (in c.m.) E_R, Γ_λ, $\Gamma_{\lambda c}$, and $\phi_c{}^R$ are also given in Table I. The target energy loss was taken as 3 keV, but this has a negligible effect on a resonance of total width $\Gamma_\lambda=80$ keV. The resonance quantum numbers were $l=0$, $j=\frac{1}{2}$.

The simultaneous fits to the eight (p,p) differential cross-section excitation functions and to the (p,n) total cross section are shown in Figs. 1–3. When fitting the data, correct shapes to the excitation functions were sought. That is, if the off-resonance cross section was too low (high) on both sides of the resonance, the best fit was taken to be the one which gave a consistently lower (higher) cross section while going through the resonance.

TABLE I. Parameters for ^{92}Zr$(p,p)^{92}$Zr and ^{92}Zr$(p,n)^{92}$Nb.

$V=53.75\pm0.5$ MeV	$r_0=1.25$ F	$E_R=5.938\pm0.005$ MeV
$W'=3.5\pm0.5$ MeV	$a=0.65$ F	$\Gamma_\lambda=80\pm6$ keV
$V_S=5.5\pm0.5$ MeV F^2	$a'=0.70$ F	$\Gamma_{\lambda c}=37\pm3$ keV
		$\phi_c{}^R=11\pm1°$

The resonance mixing phase $\phi_c{}^R$ changes the shape of the resonance. This is seen in Fig. 2, where the shapes for $\phi_c{}^R=0°$, and 11° are compared for the (p,p) excitation function at 110°. The displacement of the resonance energy discussed in Sec. II B is also observed. The value of $\phi_c{}^R$ is limited by unitarity [Eq. (32)] to be less than 35°.

In the above analyses compound elastic scattering contributions were ignored, since a Hauser-Feshbach estimate of these contributions, using the level density calculated from the composite formula of Gilbert and Cameron,[17] and the level widths in nearby ^{90}Zr measured by Fessenden *et al.*,[18] always gave much less than 1 mb/sr, which is smaller than the experimental error.

The extraction of the neutron spectroscopic factor S_n for the 0.96-MeV $\frac{1}{2}^+$ state in ^{93}Zr from the proton resonance partial width $\Gamma_{\lambda c}$ will now be described.

B. Neutron Spectroscopic Factor for the $\frac{1}{2}^+$ State at 0.96 MeV in ^{93}Zr

The neutron spectroscopic factor S_n for the lowest $\frac{1}{2}^+$ state in ^{93}Zr has been obtained previously by zero-range DWBA analysis of ^{92}Zr$(d,p)^{93}$Zr measurements.[15] The value $S_n=0.91$ has an absolute error of at least 15% due to errors in the measurement of absolute cross sections.

The theory presented in Secs. II and III enables S_n and the resonance mixing phase $\phi_c{}^R$ to be calculated from the resonance partial width $\Gamma_{\lambda c}$, the optical-model wave functions f_c (obtained from the optical-model parameters), and the neutron single-particle bound-state parameters.

Elastic scattering parameters are given in Table I. The bound-state parameters in Eq. (63) were chosen as $3s_{1/2}(l_n=0,\ j_n=\frac{1}{2})$, $\epsilon_n=5.75$ MeV (the separation energy of a neutron from the 0.96-MeV state[19]), with $r_0=1.25$ F, $a=0.65$ F, as in the proton scattering. The radial dependence of $V_n(r)$ is given in Eq. (72). If the well depth V is chosen to produce an eigenstate, one gets $V=50.0$ MeV, which is 4 MeV less than the proton-scattering value. This value is insensitive to the diffuseness. These bound-state parameters together with the (p,p) and (p,n) parameters in Table I will be referred to as the standard set.

By use of the formulas of Secs. II and III, the resonance-mixing phase and the neutron spectroscopic

[17] A. Gilbert and A. G. W. Cameron, Can. J. Phys. **43**, 1446 (1965).

[18] P. Fessenden, W. R. Gibbs, and R. B. Leachman, Phys. Rev. Letters **15**, 796 (1965).

[19] *Nuclear Data Sheets*, compiled by K. Way *et al.* (U. S. Government Printing Office, National Academy of Sciences–National Research Council, Washington 25, D. C., 1961).

TABLE II. Effects of parameter variation on S_n, R_m, and $\phi_c{}^R$ for ^{93}Zr. Standard values are $S_n=1.16$, $R_m=7.52$ F, $\phi_c{}^R=12.0°$.

Parameter varied	∇S_n	∇R_m	$\nabla\phi_c{}^R$
Neutron			
ϵ_n	6.9	0.0	0.8
r_0	− 3.3	0.1	− 1.2
a	− 1.6	0.1	− 0.8
Proton			
V	− 7.2	−1.0	− 1.0
W'	− 0.3	0.1	0.3
r_0	−10.1	−1.5	−11.1
a	− 0.2	0.1	0.3
a'	0.0	0.0	0.5

factor were calculated at $E=E_R=5.938$ MeV for the matching radius, a_c, between 6.8 and 8.0 F. The results are plotted in Fig. 4. The maximum value of $\phi_c{}^R$ for which unitarity is satisfied [see Eq. (32)] is 35°, while R_m, the radius at which S_n is a minimum, is 7.52 F. Here $S_n=1.16$, and $\phi_c{}^R=12.0°$. Within a 1-F interval centered on R_m the value of S_n varies by less than 10% from 1.16 so that the R-matrix requirement of independence of results from matching radius is nearly satisfied. The nuclear-well radius R of Eq. (76) is 5.64 F. The value of $\phi_c{}^R$ obtained from fitting the (p,p) and (p,n) data was 11° (Table I). If the matching radius a_c is chosen so that the calculated and fitted resonance-mixing phases are equal, then from Fig. 4, $a_c=7.7$ F but S_n is unchanged.

The values of S_n obtained by using the Coulomb penetrability of Eq. (35) rather than the optical penetrability of Eq. (34) are shown dashed in Fig. 4. The importance of boundary matching onto the optical-model potential region, rather than onto the Coulomb potential region, is evident.

In the present analysis the spectroscopic factor S_n changes by less than 10% for a_c between 7.0 and 8.0 F. Thus, the best choice of matching radius is not of great importance in this analysis. In general two criteria for the best value of a_c might be used: (1) The value of S_n is stationary with respect to a_c, thus satisfying the R-matrix condition of boundary-radius independence. (2) The calculated and fitted values of $\phi_c{}^R$ agree. [However, the unitarity limit, Eq. (32), on $\phi_c{}^R$ must not be violated.] In a good analysis both criteria should yield similar values for S_n.

The spreading width $W_{\lambda c}$ due to the elastic channel alone can be calculated from Eq. (60), using the optical-model parameters given in Table I, and the neutron bound-state parameters given above. The calculated value of $W_{\lambda c}/\Gamma_{\lambda c}$ is plotted against a_c in Fig. 4. Satisfactory agreement with the value obtained from Eq. (61) and the resonance parameters in Table I, $\Gamma_\lambda/\Gamma_{\lambda c}-1=1.2\pm0.2$, is observed for a_c near R_m. The calculated value may be increased by increasing the surface absorption potential W' to about 5 MeV to optimize the fit to the (p,n) cross section. However, this results in poorer fits to the (p,p) cross sections, especially at the backward angles.

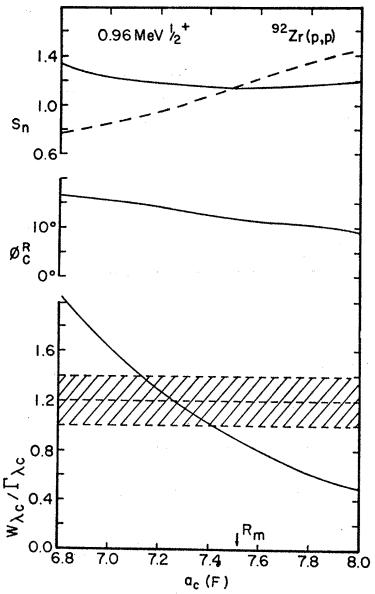

FIG. 4. Neutron spectroscopic factor S_n, resonance-mixing phase $\phi_c{}^R$, and spreading width ratio $W_{\lambda c}/\Gamma_{\lambda c}$ as a function of matching radius a_c, for 0.96-MeV $\frac{1}{2}^+$ state in ^{93}Zr. Radius where S_n is minimum, R_m. Dashed line shows S_n calculated using Coulomb penetrability. The cross-hatched area gives the measured value of $\Gamma_\lambda/\Gamma_{\lambda c}-1$.

C. Effects of Parameter Variations

Since in some cases the available data are not as complete as in the present analysis, or, as for the neutron bound state, cannot be obtained directly, it is of interest to vary the parameters of this analysis to see the effects on S_n, R_m, and $\phi_c{}^R$.

A measure of the sensitivity of the quantity q on the parameter p is the term

$$\nabla q=(\Delta q/q)/(\Delta p/p), \tag{77}$$

where Δq is the change in q for a small change Δp in p. For example, if $\nabla q=2$, then q changes by 2% for a 1% change in p. The ∇q for $q=S_n$, R_m, and $\phi_c{}^R$ are given in Table II for variations of single parameters from the standard set values. The effect of these variations on the fits to the (p,p) and (p,n) data was not investigated since such variations typically arise when data are unavailable.

However, some of the parameters can be estimated much more accurately than others. Rough estimates are for r_0, r_0', and V, 2%; for a, a', W, W', and V_S, 10%. Each of ∇S_n, ∇R_m, and $\nabla\phi_c{}^R$ should be appropriately weighted.

For the bound neutron parameters the single-particle binding energy ϵ_n may differ from the neutron separation energy since other configurations contribute to the binding. But a 10% change in ϵ_n affects S_n only about

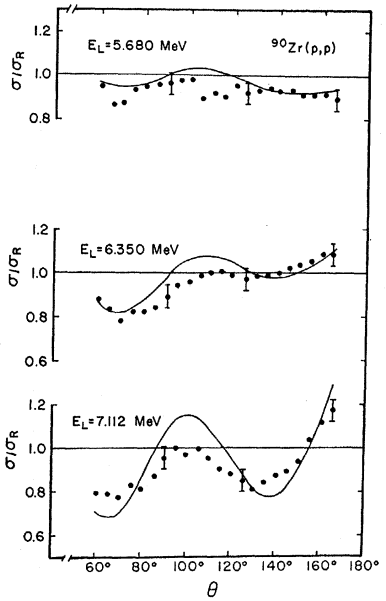

FIG. 5. Off-resonance differential cross sections $^{90}Zr(p,p)^{90}Zr$, plotted as ratio-to-Rutherford, as a function of c.m. angle θ. Absolute errors are 5%. Curves use parameters of Table III.

as much as a 2% change in r_0, or a 5% change in the diffuseness (to which S_n and $\phi_c{}^R$ are the most sensitive).

Of the proton optical-model parameters which determine S_n and $\phi_c{}^R$ for a given $\Gamma_{\lambda c}$, V and r_0 appear to produce the largest variations. However, these variations have the same sign and their effects would tend to cancel in cases of $Vr_0{}^2$ ambiguities in analysis of (p,p) data. The absorption potential W' seems, in the present analysis, to produce relatively small effects on S_n and $\phi_c{}^R$, although this may not be so in general. The spectroscopic factor is directly proportional to the partial width $\Gamma_{\lambda c}$, so that this quantity should be found as accurately as possible. Over all, the diffusenesses seem to produce the largest variations of S_n. Whether these results are generally valid for the extraction of neutron spectroscopic factors from isobaric analog states remains to be investigated.

From the above analysis and discussion, a fair estimate of the probable error in the determination of S_n from $\Gamma_{\lambda c}$ is 10%, with $\Gamma_{\lambda c}$ having an error of about 12%. Thus the $3s_{1/2}$ neutron spectroscopic factor for the 0.96-MeV state in ^{93}Zr is $S_n=1.20\pm0.2$, whereas the (d,p) value[15] of $S_n=0.91$. A qualitative comparison of the relative accuracy of the two methods will be given in Sec. VI.

V. ANALYSIS OF $^{90}Zr(p,p)^{90}Zr$ BELOW NEUTRON THRESHOLD

A. Optical-Model Parameters

Although isobaric analog resonances in the elastic scattering of protons by ^{90}Zr have been investigated previously,[20] no detailed analysis for the extraction of neutron spectroscopic factors has yet been made.

TABLE III. Parameters for $^{90}Zr(p,p)^{90}Zr$.

	$\frac{1}{2}^+$ state	$\frac{3}{2}^+$ state
$V=57.5\pm0.5$ MeV	$E_R=5.844\pm0.005$ MeV	$E_R=6.712\pm0.005$ MeV
$W'=1.25\pm0.25$ MeV	$\Gamma_\lambda=88\pm4$ keV	$\Gamma_\lambda=42\pm3$ keV
$V_S=5.5\pm0.5$ MeV F^2	$\Gamma_{\lambda c}=44\pm3$ keV	$\Gamma_{\lambda c}=16\pm2$ keV
$r_0=1.25$ F	$\phi_c{}^R=2.5°$	$\phi_c{}^R=2.5°$
$a=0.60$ F		
$a'=0.70$ F		

Differential cross-section excitation functions were available[21] for $^{90}Zr(p,p)^{90}Zr$ at lab angles of 90°, 125°, and 165°, for the lab bombarding energy range 5.7–7.0 MeV in about 20-keV steps. In this energy range occur a resonance near 5.9 MeV of which the parent analog is the 1.21-MeV $\frac{1}{2}^+$ state in ^{91}Zr, and another large resonance near 6.8 MeV with the 2.06-MeV $\frac{3}{2}^+$ state in ^{91}Zr as parent analog. In the $^{90}Zr(d,p)^{91}Zr$ reaction, two other levels in ^{91}Zr at 1.48 and 1.89 MeV are weakly populated,[15] but these are not observed (within counting statistics of about 1%) in the elastic scattering. The excitation functions are plotted as ratio-to-Rutherford in Fig. 7. The target energy loss of protons was about 18 keV near 5.9 MeV, and 17 keV near 6.8 MeV, which is much larger than the level spacing, so that the measured cross section is the quantity $\langle d\sigma/d\Omega\rangle$ of Eq. (50).

Angular distributions of the differential cross section were measured at 5.680-, 6.350-, and 7.112-MeV lab energies over the angle range 60°–165° in 5° intervals. These data are shown as ratio-to-Rutherford in Fig. 5. (Visual comparison is much more sensitive when σ/σ_R rather than σ is used.) Over-all errors of 5% were estimated for all the differential cross-section measurements.

The $^{90}Zr(p,n)^{90}Nb$ threshold is at 6.97-MeV lab energy.[19] Below this energy only (p,p') and (p,α) channels are open. However the cross sections through these channels may be negligible, since the penetrabilities are much smaller. [The Coulomb penetrability at

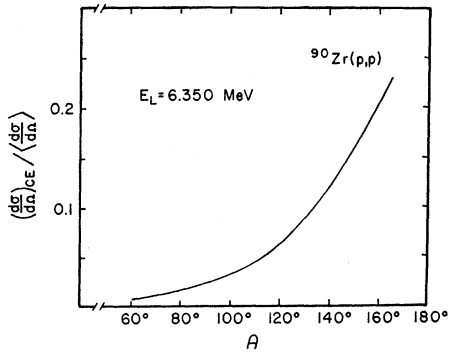

FIG. 6. Compound elastic fraction of the differential cross section for $^{90}Zr(p,p)^{90}Zr$ at lab energy 6.350 MeV, as a function of c.m. angle θ.

[20] C. F. Moore, Ph.D. dissertation, Florida State University, 1964 (unpublished).

[21] J. D. Fox (private communication).

5.8 MeV for (p,p_1) with $a_c=7$ F is a factor of 30 smaller than that for (p,p_0), but is almost equal to that for (p,p_0) at 6.8 MeV.] Therefore, compound elastic scattering can be estimated from Eq. (53).

The three angular distributions shown in Fig. 5 were analyzed using the code ANSPEC,[14] with the inclusion of the compound elastic scattering. The tails of nearby resonances contribute a few percent to the cross sections, so that previous estimates[21] of the resonance parameters were used to allow for resonance contributions. The optical-model potential used is given by Eq. (71) with the geometry parameters of Rosen *et al.*,[3] except that $a=0.60$ F rather than $a=0.65$ F was found to give better fits, as is consistent with the closed-shell nature of ^{90}Zr. The best-fit potentials, obtained by grid searches, are given in Table III and the fits are displayed in Fig. 5.

The importance of compound elastic scattering at backward angles is emphasized in Fig. 6, where the compound elastic fraction of the cross section is plotted for 6.350-MeV bombarding energy. The fraction is large even though the surface absorption potential $W'=1.25$ MeV only. Note that the potentials $V=57.5$ MeV and $W'=1.25$ MeV are significantly different from standard values[3] for which $V=51.7$ MeV and $W'=7.5$ MeV. This emphasizes the importance of measuring and analyzing off-resonance angular distributions if accurate optical-model parameters are to be used. The spreading width is very sensitive to W', but W' is not well determined below the (p,n) threshold.

B. Resonance Parameters

The differential cross-section excitation functions at 90°, 125°, and 165° are shown in Fig. 7 plotted as ratio-to-Rutherford. Previous analyses,[21] in which background scattering was ignored, and in which an arbitrary normalization between experimental yield and calculated cross section was allowed to each angle, indicated

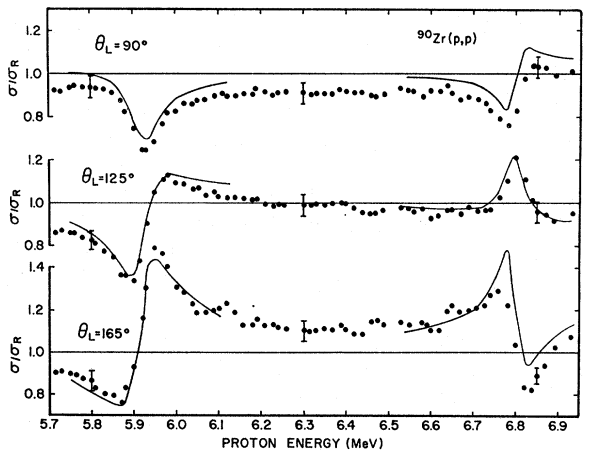

FIG. 7. Excitation function for ^{90}Zr$(p,p)^{90}$Zr at 90°, 125°, and 165°, plotted as ratio-to-Rutherford. Absolute errors are 5%. Curves use parameters in Table III.

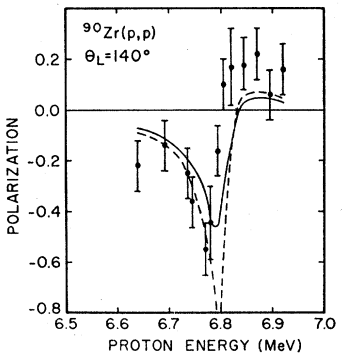

FIG. 8. Polarization excitation function for ^{90}Zr$(p,p)^{90}$Zr at 140°. Absolute errors as shown. Solid curve is P_m of Eq. (56), while dashed curve is P of Eq. (27).

that the resonance near 5.9 MeV has $l=0$, $E_R=5.800$ MeV, $\Gamma_\lambda=72$ keV, $\Gamma_{\lambda c}=32$ keV, and that the 6.8-MeV resonance has $l=2$, $j=\frac{3}{2}$, $E_R=6.700$ MeV, $\Gamma_\lambda=55$ keV, and $\Gamma_{\lambda c}=15$ keV. These estimates were used as starting values for grid searches over the resonance parameters E_R, Γ_λ, and $\Gamma_{\lambda c}$. The resonance mixing phase $\phi_c{}^R$ should be small since the absorption potential W' is small. Therefore the value $\phi_c{}^R=2.5°$, calculated from the optical-model parameters and Eq. (21), was used for both resonances. At each angle of both resonances about 20 points were used for each excitation function. If points far off resonance are used, the values of the resonance parameters may become incorrect through trying to compensate fitting discrepancies in the background-scattering estimates.

Best-fit resonance parameters are given in Table III, and the corresponding fits are shown in Fig. 7. The s-wave resonance at a lab energy of 5.918 MeV is well fitted at the three angles. However, the d-wave resonance at a lab energy of 6.796 MeV is over-all calculated too large, but this is mostly due to the overestimation of the background scattering (see Fig. 5). The large anomaly in the 125° excitation function (at this angle the non-spin-flip cross section vanishes) is due to the spin-flip cross section which includes a contribution from compound elastic scattering. Similar results have recently been reported by Gaarde *et al.*[22]

C. Polarization

Polarization data in the neighborhood of the 6.8-MeV resonance have been reported by Moore and Terrell,[23] and analyzed to extract the j value of the resonance.[10] The excitation function at a lab angle of 140° is shown in Fig. 8. The energy spread of beam and target was about 20 keV, so that the measured polarization is the quantity P_m defined by Eq. (56). With the optical-model and resonance parameters from Table III, P_m is shown as the solid curve. The polarization P, that is,

[22] C. Gaarde, K. Kemp, and P. Wilhjelm, Nucl. Phys. **A102**, 1 (1967).

[23] C. F. Moore and G. Terrell, Phys. Rev. Letters **17**, 804 (1966).

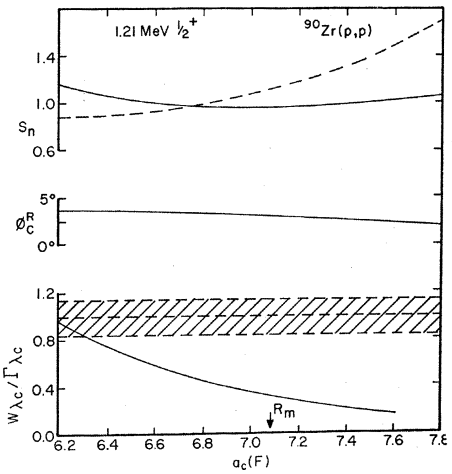

FIG. 9. Neutron spectroscopic factor S_n, resonance-mixing phase $\phi_c{}^R$, and spreading width ratio $W_{\lambda c}/\Gamma_{\lambda c}$ as a function of matching radius a_c, for 1.21-MeV $\frac{1}{2}^+$ state in ^{91}Zr. Radius where S_n is a minimum, R_m. Dashed line shows S_n calculated using Coulomb penetrability. The cross-hatched area gives the measured value of $\Gamma_\lambda/\Gamma_{\lambda c}-1$.

the polarization calculated according to Eq. (27), is shown as the dashed curve, and it is seen to be in poorer agreement with the data than is P_m. It is clear, therefore, that the polarization must be carefully defined when compound elastic scattering is significant.

From the data and fit in Fig. 8 it appears that the absolute energy calibrations of the two accelerators used for the cross-section and polarization measurements may differ by about 10 keV, since the resonance energies which best fit the cross-section and polarization data differ by about this amount. Because of this, and because the polarization errors are rather large, the polarization data were not included in the parameter fitting.

D. Neutron Spectroscopic Factors for 1.21- and 2.06-MeV States in ^{91}Zr

The neutron spectroscopic factors S_n for low-lying excited states in ^{91}Zr have been obtained by DWBA analysis of ^{90}Zr$(d,p)^{91}$Zr measurements by Cohen and Chubinsky.[15] They obtained for the $\frac{1}{2}^+$ state at 1.21 MeV, of which the s-wave resonance in ^{90}Zr$(p,p)^{90}$Zr is the analog, $S_n=0.72$. For the $\frac{3}{2}^+$ state at 2.06 MeV, whose analog is the d-wave resonance, they determined $S_n=0.45$.

Elastic scattering parameters for the present analysis are given in Table III. The bound-state parameters in Eq. (63) were taken as $3s_{1/2}$, $\epsilon_n=6.000$ MeV, and $2d_{3/2}$, $\epsilon_n=5.145$ MeV (the neutron separation energies[19]), with the same geometry as in the elastic scattering analysis. The well depths were then found to be $V=51.1$ and $V=50.3$ MeV, respectively, compared with 57.5 MeV for the proton scattering. Such differences might arise from isospin-dependent terms in the nuclear potential.

TABLE IV. Effects of parameter variation on S_n, R_m, and $\phi_c{}^R$ for ^{91}Zr. Standard values are $S_n=0.96$, $R_m=7.08$ F, $\phi_c{}^R=3.0°$ ($\frac{1}{2}^+$ state), $S_n=0.50$, $R_m=6.59$ F, $\phi_c{}^R=2.6°$ ($\frac{3}{2}^+$ state).

Parameter varied	$\frac{1}{2}^+$ state ∇S_n	∇R_m	$\nabla\phi_c{}^R$	$\frac{3}{2}^+$ state ∇S_n	∇R_m	$\nabla\phi_c{}^R$
Neutron						
ϵ_n	5.7	0.0	5.8	0.4	0.0	0.4
r_0	−3.3	0.0	−1.3	−3.2	−0.1	−1.5
a	−1.1	0.0	−0.7	−0.8	0.0	−0.6
V_S				0.1	0.0	0.0
Proton						
V	−6.5	−1.3	−4.0	−5.7	−1.4	0.0
W'	−0.5	0.0	0.7	0.0	0.0	1.0
V_S				0.2	0.0	0.0
r_0	−9.3	−1.8	−2.2	−8.4	−1.5	4.9
a	−0.3	−0.3	1.8	−0.4	0.1	0.4
a'	0.0	0.0	1.2	0.1	0.0	1.7

The formulas of Secs. II and III give the values of S_n displayed in Figs. 9 and 10 for the matching radius a_c between 6.2 and 7.8 F. The dashed line is S_n calculated using the Coulomb penetrability, Eq. (35), rather the penetrability in the optical-model potential, Eq. (34). It is seen again that for reliable spectroscopic factor estimates optical penetrabilities must be used. The minimum value of S_n is 0.96 at $R_m=7.08$ F for the $\frac{1}{2}^+$ state, and $S_n=0.50$ at $R_m=6.59$ F for the $\frac{3}{2}^+$ state. In both cases S_n varies by less than 10% within 1 F centered on R_m, and the values are in good agreement with those from the (d,p) analyses (0.72 and 0.45, respectively). The nuclear-well radius is 5.60 F.

The resonance-mixing phase $\phi_c{}^R$ was not used as a fitting parameter in this analysis, but was fixed at 2.5°. It is seen in Figs. 9 and 10 that it varies slowly with radius. The unitarity limits on $\phi_c{}^R$ are 30.5° and 33.5°.

The total spreading width $\Gamma_\lambda-\sum_c\Gamma_{\lambda c}$ should arise only from the elastic channel if the inelastic reduced widths are negligible. For the $\frac{1}{2}^+$ resonance Eq. (61) and the data of Table III result in the experimental value $\Gamma_\lambda/\Gamma_{\lambda c}-1=1.0\pm0.2$. The calculated value from Eq. (60), using the optical-model parameters of Table III, and the neutron parameters given above, is plotted versus a_c in Fig. 9. It is seen that in the neighborhood of R_m the calculated values are about half the measured values. Some of this difference is due to the inelastic channels. However W' can be increased from 1.25 to 2.0 MeV without changing S_n or the background cross section by more than a few percent, but $W_{\lambda c}/\Gamma_{\lambda c}$ increases proportionately to W' in this case. Such an increase in W' is expected if inelastic scattering is non-negligible.

The calculated spreading width ratio for the $\frac{3}{2}^+$ resonance at the higher energy near 6.8 MeV is shown in Fig. 10. It is even smaller compared with the measured value (1.6 ± 0.2) than at the $\frac{1}{2}^+$ resonance. This is to be expected since the inelastic (p,p_1) penetrability has increased from 1/30th the elastic penetrability at 5.8 MeV to nearly equal the elastic value ot 6.8 MeV.

Again the value of $W_{\lambda c}/\Gamma_{\lambda c}$ can be proportionately increased with W' without affecting S_n significantly.

The effects of parameter variations on the values of S_n, R_m, and $\phi_c{}^R$ can be investigated as in Sec. IV C. The quantities ∇S_n, ∇R_m, $\nabla\phi_c{}^R$, defined as in Eq. (77), are tabulated in Table IV for variations of single parameters from the standard set values given in Table III. Very similar effects are noticed for both the $\frac{1}{2}^+$ and $\frac{3}{2}^+$ states, with the latter being less sensitive to parameter variations. The similarity with Table II for the ^{93}Zr $\frac{1}{2}^+$ state should also be noted. When $\Gamma_{\lambda c}$ or $\Gamma_{\lambda c}/\Gamma_\lambda$ is small, errors in fitting the resonance excitation function are significant. Usually $\Gamma_{\lambda c}$ can be determined to within 2 keV. This would lead to an error of 12% for the $\frac{3}{2}^+$ state which has $\Gamma_{\lambda c}=16$ keV.

The value of the neutron spectroscopic factor for the 1.21-MeV $\frac{1}{2}^+$ state in ^{91}Zr is estimated as $S_n=0.95\pm0.15$, and for the 2.06-MeV $\frac{3}{2}^+$ state in ^{91}Zr, $S_n=0.50\pm0.08$.

VI. COMPARISON OF (p,p) ANALOG RESONANCE AND (d,p) STRIPPING METHODS

A comparison of the reliability of the analog state (p,p) resonance method with that for the (d,p) stripping reaction method for the extraction of neutron spectroscopic factors is difficult to make because of the very different techniques employed. However, the comparison may be broadly grouped according to the data required, the validity of the reaction model, the sensitivity of the results to ill-determined parameters, and the dependence of the measurements on the spectroscopic factor.

The data needed for the (p,p) method are elastic scattering excitation functions near the analog resonance measured at each of a few angles, and off-resonance (p,p) differential cross sections. Also, total (p,n) cross sections are often very helpful in determining the optical-model parameters. The proton energy for excitation of analogs of low-lying states can be reliably estimated from Coulomb energy systematics, and is seldom far above the Coulomb barrier. Therefore only the resonant scattering in a single proton channel produces a large anomaly and the l value of this channel (and hence of the parent analog neutron) is readily determined from the angular dependence of the anomaly. The j value can then be determined from analysis of a rough polarization measurement.[10] Data on the (p,n) absolute cross sections for the same resonance are helpful for estimates of the resonance parameters. This is especially important since below the Coulomb barrier the elastic scattering angular distributions may have little structure and, therefore, be insensitive to the nuclear potential parameters.

The (d,p) method requires angular-distribution data on (d,d) from the target and (p,p) from the residual nucleus (which is unstable for excited neutron states, and often also for the ground state), in addition to data on the (d,p) reaction itself. The neutron l value is readily determined from the angular dependence of (d,p) only when entrance- and exit-channel scattering effects are small. There is no clear way of determining the j value, although small but systematic j-dependent effects have been revealed in differential cross-section measurements.[24,25] These effects become much more pronounced in (d,p) when polarization measurements are performed,[26] as in the (p,p) situation.

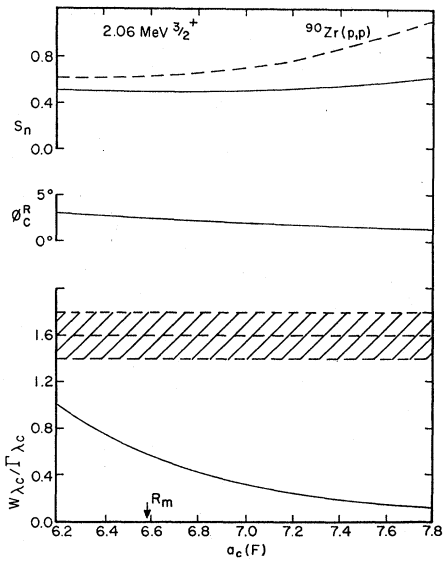

FIG. 10. Neutron spectroscopic factor S_n, resonance-mixing phase $\phi_c{}^R$, and spreading width ratio $W_{\lambda c}/\Gamma_{\lambda c}$ as a function of matching radius a_c, for 2.06-MeV $\frac{3}{2}^+$ state in ^{91}Zr. Radius where S_n is a minimum, R_m. Dashed line shows S_n calculated using Coulomb penetrability. The cross-hatched area gives the measured value of $\Gamma_\lambda/\Gamma_{\lambda c}-1$.

The reaction model employed in the (p,p) analysis is model-dependent primarily in that the background scattering is calculated using an optical-model potential to account for the effects of the nonelastic channels on the elastic channel. In calculating the effect of the background scattering on the resonance amplitude, Eqs. (7) and (15) ignore some of the off-diagonal elements of the background R matrix, $\mathbf{R}^0$, above thresholds. The splitting of the R matrix into background and resonance terms may not be unique, but this may be accounted for by the optical penetrability, Eq. (34), which modifies the resonance partial width appropriately. In the extraction of the neutron spectroscopic factor, the choice of a charge-independence matching radius a_c may be ambiguous. The (p,p) analysis places major emphasis on the resonance effects in the interaction.

For the (d,p) method a zero-range DWBA calculation is usually made. The inclusion of finite-range effects, antisymmetrization, channel coupling in the

[24] L. L. Lee, Jr., and J. P. Schiffer, Phys. Rev. Letters **12**, 108 (1964).

[25] J. P. Schiffer, L. L. Lee, Jr., A. Marinov, and C. Mayer-Böricke, Phys. Rev. **147**, 829 (1966).

[26] T. J. Yule and W. Haeberli, Phys. Rev. Letters **19**, 756 (1967).

entrance and exit channels, or compound-nucleus effects is seldom attempted. Both the (d,d) and (p,p) scattering use an optical-model potential, and the contributions of off-diagonal terms in these scatterings are ignored in calculating (d,p). A measurement and analysis of $^{90}Zr(d,p)^{91}Zr$ proton polarization with 11-MeV deuterons[27] finds reasonable agreement between DWBA predictions of the cross section and the measured cross section, but considerable disagreement for the polarizations. The use of DWBA for contributions from the nuclear interior may be a poor approximation, so that the interior contributions are often conveniently ignored by use of an arbitrary radial cutoff [as in the $^{92}Zr(d,p)^{93}Zr$ analysis[15] which is compared with the (p,p) method here]. Thus, in contrast to the (p,p) analysis, emphasis is placed on a nonresonance mechanism, rather than a resonance mechanism.

It is important for the extraction of nuclear-structure information that the method of analysis, when applied to a particular case, yields results which are insensitive to ill-determined parameters, and to approximations made in the reaction model, but very sensitive to the quantities to be extracted. For the (p,p) isobaric analog resonance analysis presented here, it was found that the fits were sensitive to the potential parameters. Thus for reliable results, the optical-model parameters should be determined from the (p,p) and (p,n) data, rather than estimated from a standard set. The diffuseness (both in the optical-model potential and in the neutron bound state) probably contributes the largest uncertainty in the value of the spectroscopic factor S_n.

The sensitivity of the (d,p) analyses to the parameter uncertainties and to the reaction-model approximations have been investigated by Smith[28] for $^{90}Zr(d,p)^{91}Zr$, and by Lee *et al.*[29] for $^{40}Ca(d,p)^{41}Ca$. Since, unlike the analog-state method, the spectroscopic factor is a normalization factor between the experimental cross section (typically 5 mb/sr) and the calculated angular distribution, it is very sensitive to magnitude changes induced by parameter variations, as well as the large over-all normalization errors in the experimental data. The deuteron wave function overlap is also part of the normalization and may be uncertain by 30% or more.[7] These effects have been discussed in detail in Refs. 28 and 29. Moreover, the (d,p) cross sections may be much more sensitive to the optical-model parameters than are those for (d,d) and (p,p) separately. Smith,[28] in a detailed study of $^{90}Zr(d,p)^{91}Zr$ using DWBA, found factors of 2 between spectroscopic factors for different deuteron and proton parameter sets which fit the elastic scattering data.

In conclusion, the simplicity of the isobaric analog resonance elastic scattering measurement and the R-matrix analysis for the extraction of neutron spectroscopic factors of low-lying bound states in medium to heavy nuclei should be realized. Compared with the (d,p) methods, the data requirements are less, the reaction model is more exact (yet easy to calculate), and the number of parameters is fewer. Therefore systematic analyses of (p,p) analog resonances by the experimental and analytic techniques suggested here should contribute greatly to precise nuclear-structure information.

ACKNOWLEDGMENTS

The cooperation of Dr. J. D. Fox in providing the $^{92}Zr(p,p)^{92}Zr$, $^{92}Zr(p,n)^{92}Nb$, and $^{90}Zr(p,p)^{90}Zr$ data is acknowledged. Computer facilities were provided by the Florida State University Computing Center.

[27] L. S. Michelman, E. J. Ludwig, S. Fiarman, and A. B. Robbins, Bull. Am. Phys. Soc. 12, 527 (1967).
[28] W. R. Smith, Phys. Rev. 137, B913 (1965).
[29] L. L. Lee, Jr., J. P. Schiffer, B. Zeidman, G. R. Satchler, R. M. Drisko, and R. H. Bassel, Phys. Rev. 136, B971 (1964).